Mode specific dynamics in bond selective reaction $O'(^3P) + HOD \rightarrow O'H + OD/O'D + OH$

Rui Zheng, Yongfa Zhu, and Hongwei Song

Citation: The Journal of Chemical Physics **149**, 054304 (2018); doi: 10.1063/1.5037492
View online: https://doi.org/10.1063/1.5037492
View Table of Contents: http://aip.scitation.org/toc/jcp/149/5
Published by the American Institute of Physics

Mode specific dynamics in bond selective reaction $O'(^3P) + HOD \rightarrow O'H + OD/O'D + OH$

Rui Zheng,[1,2] Yongfa Zhu,[2,3] and Hongwei Song[2,a)]
[1]*School of Mathematics and Statistics, North China University of Water Resources and Electric Power, Zhengzhou 450011, China*
[2]*State Key Laboratory of Magnetic Resonance and Atomic and Molecular Physics, Wuhan Institute of Physics and Mathematics, Chinese Academy of Sciences, Wuhan 430071, China*
[3]*University of Chinese Academy of Sciences, Beijing 100049, China*

(Received 24 April 2018; accepted 20 July 2018; published online 6 August 2018)

Taking advantage of bond selectivity and mode specificity has long been realized to control the outcome of chemical reactions. The mode-specific dynamics in the bond selective abstraction reaction $O'(^3P) + HOD$ are investigated using a full-dimensional time-dependent quantum wave packet method. Integral cross sections and product branching ratios from several low-lying vibrational states of the reactant HOD are calculated on an accurate global potential energy surface describing the lowest triplet state of the HOOH system. Both the H-abstraction reaction and the D-abstraction reaction prefer the vibrational energy to the translational energy, satisfying the prediction of Polanyi rules for a late-barrier reaction. The observed strong bond selectivity can be rationalized by the sudden vector projection model as well. The bias to the D-abstraction channel for the reaction $O'(^3P) + HOD$ from the reactant ground state can be partially attributed to the different mass combination in comparison to the H + HOD reaction, in which the H-abstraction channel is more favored. *Published by AIP Publishing.* https://doi.org/10.1063/1.5037492

I. INTRODUCTION

Control of chemical reactions is one of the most important goals in chemistry research.[1–4] Traditionally, the reactivity of a reaction is controlled by changing external conditions or introducing catalysts. However, the widely existing mode specificity in activated chemical reactions provides a new and appealing choice to achieve the goal.[1,2,5,6] The relative efficacy of the vibrational and translational modes in promoting a reaction can be qualitatively predicted by Polanyi rules,[7,8] which state that vibrational energy is more efficient in promoting a late-barrier reaction than translational energy while translational energy becomes more efficient in an early-barrier reaction, and quantitatively determined by the recently proposed sudden vector projection (SVP) model,[9,10] in which the efficacy of a reactant mode in enhancing a reaction is attributed to its coupling with the reaction coordinate at the transition state.

If the energy randomization of a reactant via the intramolecular vibrational energy redistribution (IVR) is not too fast, one could insert a chemically significant amount of energy in the bond along the reaction coordinate to boost production. The scheme has been successfully applied to bimolecular chemical reactions involving typical local-mode molecules, such as H_2O.[5,11–19] Crim, Zare, and their co-workerss have experimentally studied the reactions between H, O, or Cl and H_2O or the partially deuterated water (HOD), in which the product branching ratios and rotational and vibrational state distributions were measured.[11–17,19]

Theoretically, the bond selective dynamics have been investigated at different levels of theory, including quasi-classical trajectory (QCT)[20–22] and quantum dynamics (QD) models with either reduced[23–26] or full dimensionality.[27–36] Fu and Zhang[35] carried out exact QD calculations of the H + HOD abstraction reaction and reproduced strong bond-selective effects. The mode specificities and product branching ratios in the F/Cl + HOD reactions were studied by Song *et al.*[32–34] using QD and/or QCT methods. The feature of strong bond selectivity was found in the two reactions as well. In this work, the dynamics of the $O(^3P)$ + HOD reaction on the lowest triplet state of the HOOH system will be studied to advance our understanding of the mode specificity and bond selectivity in the prototypical X + HOD (X = H, F, Cl, $O(^3P)$) reactions.

Several global potential energy surfaces (PESs) describing the collision between $O(^3P)$ and $H_2O(^1A_1)$ have been reported since the first non-reactive PES by Redmon *et al.*[37] Braunstein *et al.*[38] built PESs for the three lowest triplet states of the HOOH system to describe the reaction $O(^3P) + H_2O(^1A_1) \rightarrow OH(X^2\Pi) + OH\ (X^2\Pi)$, which were spline-based fits of ~20 000 *ab initio* points at the complete-active-space self-consistent field plus second-order Møller-Plesset perturbation theory (CASSCF+MP2) level with a $O(4s3p2d1f)/H(3s2p)$ one electron basis set. Then, Conforti *et al.*[39] computed ~100 000 *ab initio* points at the same level of theory and basis set to fit the PESs employing the permutationally invariant polynomials (PIPs).[40,41] The PESs include both the OH + OH hydrogen abstraction channel and the

a)Author to whom correspondence should be addressed: hwsong@wipm.ac.cn

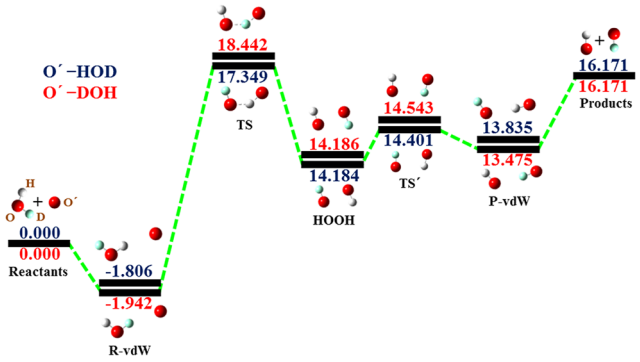

FIG. 1. Schematic illustration of the zero-point energy corrected reaction pathways for the two abstraction channels of the O′(^{3}P) + HOD reaction. O′-HOD represents the attacking atom O′ toward the atom H of HOD, while O′-HOD denotes the atom O′ toward the atom D of HOD.

H + OOH hydrogen elimination channel. However, the $1^3A''$ PES underestimates the activation and reaction energies for the OH + OH channel by 3-4 kcal mol^{-1}. Li and Guo[42] developed an accurate PES for the lowest triplet state of HOOH ($1^3A''$) by fitting more than 36 000 *ab initio* points at the level of the unrestricted coupled-cluster singles, doubles, and perturbative triples method with an augmented valence triple zeta basis set using both the PIP and permutationally invariant polynomial-neural network (PIP-NN) methods.[43] The PES reproduces well the benchmark barrier height and experimental reaction endothermicity. Recently, Li and co-workers[44] constructed a new multi-channel global PES by fitting ~28 000 *ab initio* points at the level of the explicitly correlated version of the multi-reference configuration interaction (MRCI-F12) theory using the PIP-NN method,[45] which covers the OH + OH channel, H + HO_2 channel, and the H_2 + O_2 channel on the lowest triplet state of HOOH and has a total root mean square fitting error (RMSE) of 6.7 meV. Kinetic and dynamics studies have been carried out on these PESs and the results have been compared with available experimental data.[30,36,38,42,44,46,47]

The initial state selected time-dependent quantum wave packet method will be employed to study the mode-specific dynamics in the bond selective reaction O′(^{3}P) + HOD → O′H + OD/O′D + OH. The PES of the lowest triplet state of the HOOH system developed by Li *et al.*[43] is adopted in the dynamics calculations due to the small RMSE of only 0.8 meV. The zero-point energy (ZPE) corrected reaction pathways for the two abstraction channels of the O′(^{3}P) + HOD reaction are displayed in Fig. 1. We hope to gain a comprehensive insight into the bond selectivity and mode specificity in the prototypical X + HOD (X = H, F, Cl, O(^{3}P)) reactions. The paper is organized as follows. Section II introduces briefly the theoretical methodology, followed by results and discussions in Sec. III. Conclusions are given in Sec. IV.

II. THEORY

The initial state-selected time-dependent wave packet method has been detailed in the literature.[48,49] Here, we only briefly outline the theoretical aspects related to this work. The six-dimensional Hamiltonian in the reactant atom-triatom Jacobi coordinates, as shown in Fig. 2, for a given total angular momentum J can be written as ($\hbar$ = 1 thereafter)[48]

$$\hat{H} = -\frac{1}{2\mu_R}\frac{\partial^2}{\partial R^2} - \frac{1}{2\mu_1}\frac{\partial^2}{\partial r_1^2} - \frac{1}{2\mu_2}\frac{\partial^2}{\partial r_2^2} + \frac{(\hat{J}-\hat{j}_{12})^2}{2\mu_R R^2} + \frac{\hat{l}_1^2}{2\mu_1 r_1^2} + \frac{\hat{j}_2^2}{2\mu_2 r_2^2} + \hat{V}(R, r_1, r_2, \theta_1, \theta_2, \varphi_1), \quad (1)$$

where μ_R, μ_1, and μ_2 are reduced masses of the moieties O_A-$H_BO_CD_D$, H_B-O_CD_D, and O_CD_D. $\hat{j}_2$ is the rotational angular momentum operator of O_CD_D, $\hat{l}_1$ is the orbital angular momentum operator of the atom H_B with respect to O_CD_D, and $\hat{j}_{12} = \hat{l}_1 + \hat{j}_2$ is the angular momentum operator of $H_BO_CD_D$.

The basis functions employed to expand the total wavefunction are the same as those in Ref. 49. The centrifugal-sudden (CS) approximation[50,51] has been widely applied to activated reactions to reduce the computational cost.[52–57] This approximation generally works well in direct reactions although visible differences between the CS and coupled-channel integral cross sections (ICSs) at high collision energies have been reported in the H + H_2O → H_2 + OH reaction.[31] Under the CS approximation, the centrifugal term in the Hamiltonian, $\left(\hat{J}-\hat{j}_{12}\right)^2$, is approximate to

$$\left\langle \Phi_{jK}^{JM\varepsilon} \middle| (\hat{J}-\hat{j}_{12})^2 \middle| \Phi_{j'K'}^{JM\varepsilon} \right\rangle \approx \delta_{jj'}\delta_{KK'}\left[J(J+1) + j_{12}(j_{12}+1) - 2K^2\right]. \quad (2)$$

The quantum dynamics calculations thereafter are carried out using the CS approximation. Note that the existence of the pre-reaction van der Waals well possibly introduces some error into the calculations under the CS approximation.

The initial wave packet $|\chi\rangle$ is constructed as the direct product of a localized Gaussian wave packet along the scattering coordinate R and a specific rovibrational state of the reactant HOD in the BF representation,

$$|\chi\rangle = \left(\frac{1}{\pi\delta^2}\right)^{1/4} e^{-(R-R_0)^2/2\delta^2} e^{-ik_iR} |v_0 j_{120}\tau; J\varepsilon\rangle, \quad (3)$$

where R_0 and δ are the mean position and width of the Gaussian function and k_i is the mean momentum given by E_i via $E_i = \sqrt{2\mu_R E_i}$. v_0, j_{120}, and τ represent the initial vibrational state, the initial rotational state, and the parity of the reactant HOD, respectively. The second-order split-operator method is implemented to propagate the wave packet.[58] To prevent the artificial reflection of the wave packet from the boundaries, the negative imaginary absorbing potentials $D(x) = -i\alpha(\frac{x-x_a}{x_{max}-x_a})^n$ are applied at the grid edges, in which

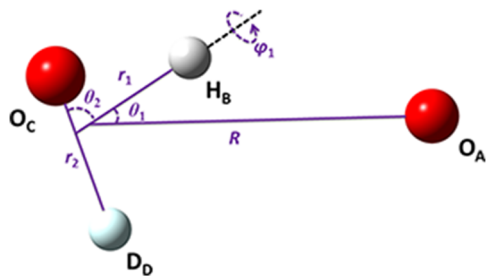

FIG. 2. The six-dimensional Jacobi coordinates for the A + BCD system.

$x = R$, r_1 and r_2, x_a is the starting point of the absorbing potential.[59]

The total reaction probability from a specified rovibrational state of HOD is calculated using the flux formula

$$P^{J\varepsilon}_{v_0 j_{120}\tau}(E) = \left\langle \psi_i^+(E) \middle| \hat{F} \middle| \psi_i^+(E) \right\rangle, \tag{4}$$

where $\hat{F}$ are the flux operators defined in the two product channels.[60] v_0, j_{120}, and τ represent the initial vibrational state, the initial rotational state, and the parity of the reactant HOD, respectively. The time-independent scattering wavefunction, $\psi_i^+(E)$, is obtained by Fourier transforming the time-dependent wavefunction at the corresponding dividing surface. The integral cross section (ICS) is obtained by summing the reaction probabilities over all relevant partial waves,

$$\sigma_{v_0 j_{120}\tau}(E_c) = \frac{1}{(2j_{120}+1)} \frac{\pi}{2\mu_R E_c} \times \sum_{K_0\varepsilon} \sum_{J \geq K_0} (2J+1) P^{J\varepsilon}_{v_0 J_{120}\tau K_0}(E_c). \tag{5}$$

The initial state-specific rate constant is obtained by thermal averaging the collision energy of the corresponding integral cross section as

$$k_{v_0 j_{120}\tau}(T) = \sqrt{\frac{8k_bT}{\pi\mu}} \frac{1}{(k_bT)^2} \int_0^\infty dE_c E_c \times \exp(-E_c/K_bT) \sigma_{v_0 j_{120}\tau}(E_c). \tag{6}$$

Since we are only interested in the vibrationally excited reactant HOD in this study, the angular momentum index is dropped off thereafter.

III. RESULTS AND DISCUSSION

The numerical parameters on an L-shaped grid[61] are listed in Table I. For the scattering coordinate R, 118 sine discrete variable representation (DVR) grid points/basis functions[62] are used in the asymptotic region and 58 in the interaction region. For the dissociating bond r_1 (r_2), 27 (37) potential optimized DVR (PODVR) grid points/basis functions[63] are employed in the interaction region and 3 (3) in the asymptotic region. The maximum values of l_1 and j_2 are determined to be 46. The flux dividing surfaces are positioned at $r_1^F = r_2^F = 3.2$ bohrs. The initial wave packet is centered at 11.0 bohrs and the propagation time is around 30 000 a.u. The vibrational states of the reactant HOD are assigned as (v_{OD}, v_b, v_{OH}), in which the three quantum numbers in the parentheses denote excitations in the OD stretching mode, the bending mode, and the OH stretching mode, respectively. The calculated fundamentals of the three modes v_{OD},v_b, and v_{OH}, are 2717.01, 1396.60, and 3718.86 cm^{-1}, consistent with experimental values of 2726.73, 1402.20, and 3707.47 cm^{-1}.[64]

TABLE I. Numerical parameters used in the wave packet calculations. (Atomic units are used unless stated otherwise.)

	O′ + HOD
Grid/basis range and size:	$R \in [2.5, 13.5]$, $N_R{}^{tot} = 176, N_R{}^{int} = 58$ $N_{r_1}{}^{int} = 27, N_{r_1}{}^{asy} = 3$ $N_{r_2}{}^{int} = 37, N_{r_2}{}^{asy} = 3$ $l_{1max} = 46, j_{2max} = 46$
Initial wave packet:	$R_0 = 11.0, \delta = 0.65, E_i = 0.15$ eV
Damping term:	$R_a = 11.0, \alpha_R = 0.05, n_R = 1.5$ $r_{1a} = 3.8, \alpha_{r_1} = 0.05, n_{r_1} = 1.5$ $r_{2a} = 3.8, \alpha_{r_2} = 0.05, n_{r_2} = 1.5$
Flux position:	$r_1{}^F = 3.2, r_2{}^F = 3.2$

A. Mode specificity

Figure 3 shows the calculated integral cross sections (ICSs) of the H-abstraction reaction O′(^{3}P) + HOD → O′H + OD from the first five vibrational states of HOD as a function of translational energy in the upper panel and total energy in the lower panel. The total energy is referred to the reactant asymptote. It can be seen in the upper panel that from each initial state the ICS increases monotonically from the energy threshold with the collision energy, satisfying the activation nature of the reaction. When the reactant HOD is vibrationally excited, the energy threshold is shifted to lower energy and the ICS becomes larger. Thus, excitations of the three modes of HOD all promote the reaction, in which exciting the OH stretching mode presents the strongest promotional effect while exciting the OD stretching mode has the weakest effect. It can be understood as follows. On one hand, the vibrational energy of the OH stretching mode is visibly higher than that of the OD stretching mode and the HOD bending mode. On the other hand, the OH stretching motion is actually along the reaction coordinate of the O′(^{3}P) + HOD → O′H + OD reaction. The vibrational energy deposited in the OH stretching mode will

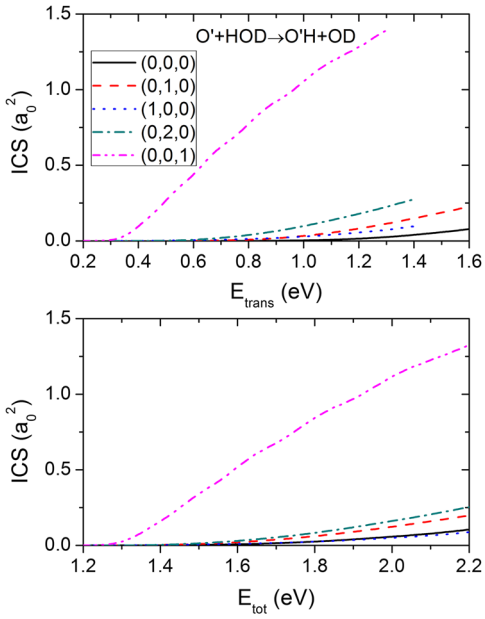

FIG. 3. ICSs of the O′(^{3}P) + HOD → O′H + OD reaction from the first five vibrational states of HOD as a function of translational energy (upper panel) and total energy (lower panel).

mostly flow into the reaction coordinate to accelerate the reaction due to the strong local mode character of the reactant HOD.

In the lower panel of Fig. 3, clearly, the vibrational energy initially deposited in the OH stretching mode promotes the reaction much more than the same amount of vibrational energy deposited in the bending mode. And the vibrational energy in both the OH stretching mode and the bending mode is more efficient than the translational energy in enhancing the reaction, in agreement with the prediction of Polanyi rules[7,8] for a late-barrier reaction. Furthermore, the promotional effect of the OD vibration is comparable to the translational energy, indicating that the OD bond is not an ideal spectator bond due to the small but nonnegligible interbond coupling.

For the D-abstraction reaction O′(^{3}P) + HOD → O′D + OH, the ICSs are displayed in Fig. 4. The mode specificity is to some extent similar to the H-abstraction reaction. Exciting the stretching mode of the bond OD greatly enhances the cleavage of the bond. Vibrational excitation of the other modes of HOD promotes the reaction as well. However, they are not as efficient as the OD stretching mode. From the lower panel, it can be found that the vibrational energy deposited in the OD stretching mode is much more efficient than the translational energy in promoting the reaction while fundamental excitation of the bending mode has comparable efficacy to the translational energy. In addition, the vibrational energy in the OH stretching mode is less efficient than the translational energy. More impressively, when the reactant HOD is excited to the first overtone state of the bending mode, the vibrational energy becomes remarkably more efficient than the same amount of translational energy. There possibly exists a reaction mechanism change from the fundamental excitation of the bending mode to the first overtone excitation, due to which the vibrational energy in the bending mode flows more easily into the reaction coordinate. We note in passing that Zhao *et al.*[65] argued that the enhancement effect was caused by a 1:2 Fermi resonance between the fundamental OD stretching mode and the first overtone of the bending mode. The dynamical behavior reminds us that it sometimes may be insufficient to describe the mode specificity simply according to the kind of the energy.

Since no matter the H-abstraction or the D-abstraction they both produce the same molecules OH and OD, adding the two product channels together would be more meaningful from the viewpoint of experiments where the internal states of OH and OD are not resolved (e.g., those addressed to measure ICSs or rate constants). Figure 5 depicts the total ICSs of the reaction O′(^{3}P) + HOD to both the O′H + OD and O′D + OH channels. As expected, vibrational energy is more favored in promoting the reaction than translational energy. The efficacy ranking for the three vibrational modes is $v_{OH} > v_{OD} > v_b$ over the energy range interested. Note that the fundamental of the OH stretching mode is about 1000 cm^{-1} larger than that of the OD stretching mode.

The relative efficacy of different reactant modes in the two abstraction channels can be partially rationalized by the aforementioned SVP model.[9,10] The SVP model takes the advantage of the fact that the IVR in reactant molecules is generally much slower than the collision time. In the sudden limit, the efficacy of a reactant mode in promoting a reaction is reasonably represented by the projection of its normal vector ($\vec{Q}_i$) onto the reaction coordinate vector ($\vec{Q}_{RC}$) at the transition state: $P_i = \vec{Q}_i \cdot \vec{Q}_{RC} \in [0, 1]$.

Table II lists the calculated SVP values. For the H-abstraction channel, the OH stretching mode has the largest projection of 0.99, which is followed by the OD stretching mode of 0.08 and the translational mode of 0.05. These projections indicate that the OH stretching motion is actually along

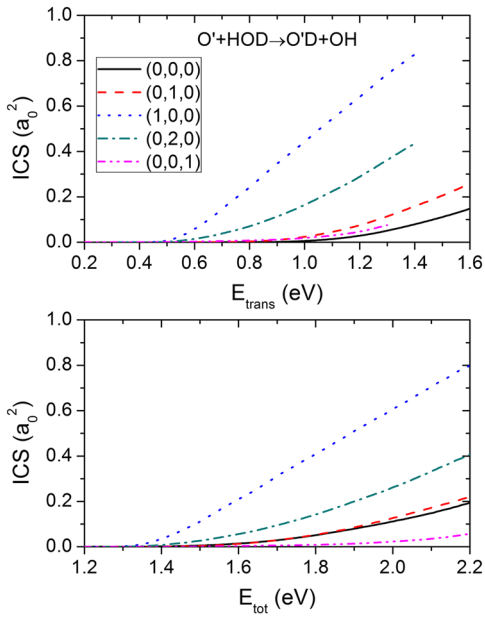

FIG. 4. ICSs of the O′(^{3}P) + HOD → O′D + OH reaction from the first five vibrational states of HOD as a function of translational energy (upper panel) and total energy (lower panel).

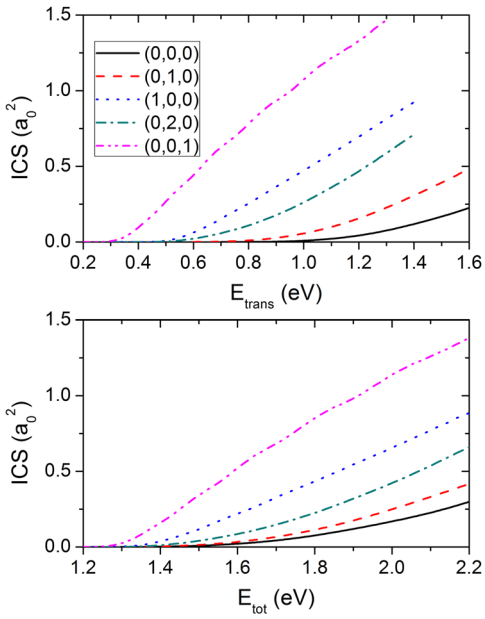

FIG. 5. ICSs of the O′(^{3}P) + HOD reaction to the two product channels O′H + OD and O′D + OH from the first five vibrational states of HOD as a function of translational energy (upper panel) and total energy (lower panel).

TABLE II. SVP values for the O′ + HOD reaction.

	SVP	
Species	O′ + HOD → O′H + OD	O′ + HOD → O′D + OH
v_{OD}	0.08	0.99
v_b	0.03	0.02
v_{OH}	0.99	0.04
Trans	0.05	0.09

the H-abstraction reaction coordinate and exciting the OH stretching mode promotes the reaction much more than exciting the OD stretching mode or increasing the same amount of translational energy, which agree well with the QD results. However, the QD calculations show that the vibrational energy deposited in the bending mode enhances the reaction slightly more than the translational energy. This behavior cannot be correctly predicted by the SVP model as the projection of v_b is smaller than the value of the translational mode. The enhancement of exciting the bending mode is partly caused by the mode softening. The bending mode softens in response to chemical forces near the transition state when the atom O approaches HOD, leading to a lowered adiabatic barrier. The reduction of the barrier is 1.97 kcal/mol for the H-abstraction channel and 1.43 kcal/mol for the D-abstraction channel with respect to the ZPE corrected barrier. For the D-abstraction channel, the OD stretching mode moves along the reaction coordinate at the transition state, as inferred by the largest projection of 0.99. The OH stretching mode gives a projection of 0.04, which is smaller than the value of the translational mode. Therefore, the efficiency of the translational mode in promoting the reaction is in between the OD stretching mode and the OH stretching mode, which is in accord with the QD calculations.

Figure 6 shows the initial state-selected rate constants to both channels. The corresponding values at several representative temperatures are listed in Table III. Unfortunately, there are no experimental data available. It can be noted that the rate constants are very small at room temperature due to the significant barrier of the reaction. As the temperature increases, the rate constant raises very sharply.

B. Isotopic branching ratio

The collision energy dependence of the product branching ratio of the H-abstraction reaction and the D-abstraction reaction is presented in Fig. 7. The corresponding values at several

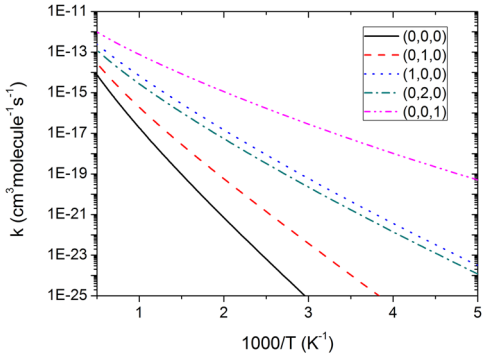

FIG. 6. Initial state-specific rate constants of the O + HOD reaction from several low-lying vibrational states of the reactant HOD.

selected translational energies are given in Table IV. From the ground state of HOD, the O′D:O′H ratio (O′ denotes the attacking oxygen atom) increases from a value of 1.37 with the collision energy and becomes nearly unchanged around 1.85 at high collision energies. It means that the reaction O′ + HOD from the ground state of HOD favors the D-abstraction channel. Fundamental excitation of the bending mode alters the bias. The H-abstraction channel is then more preferred at low collision energies and yet the yields of the two channels become comparable as the collision energy increases up to 1.3 eV. First overtone excitation of the bending mode gives rise to a similar trend of the ratio to that from the ground state except that the reaction occurs at lower energies. In addition, unsurprisingly, excitation of the local stretching mode significantly increases the yield of the corresponding product channel. For the fundamental excitation of the OD bond, the ratio first increases from a value of 5.31 with the collision energy, reaches a maximum of 19.80, and then starts to decrease as the collision energy further increases. By contrast, when the OH bond is excited to the fundamental state, the O′H:O′D ratio (the reciprocal of the O′D:O′H ratio in Fig. 7) decreases monotonically from 242.67 to 18.63 with the increase of the collision energy.

To delve into the different reactivity of the H-abstraction channel and the D-abstraction channel in the O′ + HOD reaction, the opacity functions from the ground rovibrational state of HOD are plotted in Fig. 8 with the collision energy fixed at 1.0 eV, 1.2 eV, and 1.6 eV. The value of total angular momentum J_{tot} is considered as the counterpart of the impact parameter in the classical collision theory. It can be seen that for each selected collision energy, the opacity functions of the two

TABLE III. Initial state-specific rate constants (in cm^3 molecule^{-1} s^{-1}) of the O′ + HOD reaction.

Temp (K)	(000)	(010)	(100)	(020)	(001)
200	2.00×10^{-33}	2.73×10^{-29}	3.13×10^{-24}	1.19×10^{-24}	5.09×10^{-20}
300	3.55×10^{-27}	3.46×10^{-24}	1.05×10^{-20}	4.00×10^{-21}	9.10×10^{-18}
500	7.05×10^{-22}	5.81×10^{-20}	1.48×10^{-17}	5.47×10^{-18}	1.13×10^{-15}
1000	1.88×10^{-17}	1.93×10^{-16}	6.88×10^{-15}	2.76×10^{-15}	7.68×10^{-14}
1500	9.20×10^{-16}	4.71×10^{-15}	6.96×10^{-14}	3.18×10^{-14}	3.95×10^{-13}
2000	7.64×10^{-15}	2.83×10^{-14}	2.46×10^{-13}	1.26×10^{-13}	9.82×10^{-13}

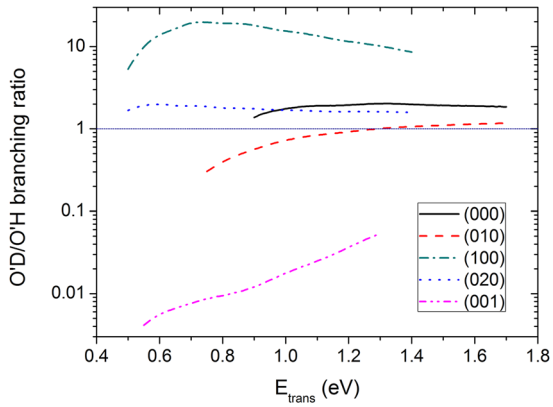

FIG. 7. Product branching ratios of the O′D + OH channel and the O′H + OD channel as a function of translational energy.

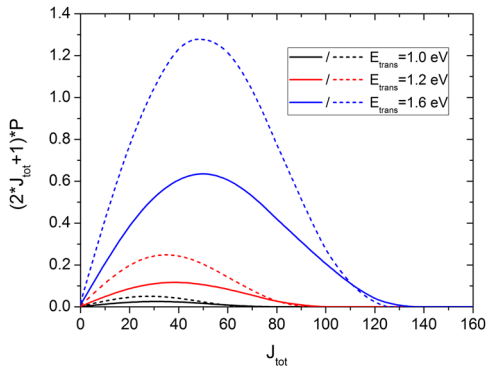

FIG. 8. Opacity functions of the O′D + OH channel and the O′H + OD channel from the ground rovibrational state of the reactant HOD with the collision energy fixed at 1.0 eV, 1.2 eV, and 1.6 eV. The solid lines denote the H-abstraction channel while the dashed lines represent the D-abstraction channel.

channels span nearly the same range of J_{tot} although the magnitude of the D-abstraction channel is significantly larger than that of the H-abstraction channel. Therefore, the preference to the D-abstraction channel from the ground state cannot be attributed to the enlargement of the cone of acceptance with respect to the H-abstraction channel. We also examine the opacity functions from the other initial states and the distributions of the two channels close to each other as well.

The bond selectivity in the prototypical reactions X + HOD (X = H, F, Cl) has been thoroughly studied in the past. It has been realized that exciting the local stretching mode dramatically facilitates the cleavage of the corresponding bond.[32,34,35] The O′(^{3}P) + HOD reaction shows analogical characters with these reactions. However, the product branching ratios from the ground rovibrational state of HOD differ from each other. It is expected that the H-abstraction channel will be more favored than the D-abstraction channel due to the lower vibrationally adiabatic barrier height. However, the preference to the product OD is only observed in the H/F + HOD reactions.[32,35] The schematic diagrams of the minimum energy paths (MEPs) of the four reactions X + H_2O (X = H, F, Cl, O(^{3}P)) are referred to Ref. 36. The abstraction reactions H/Cl/O(^{3}P) + H_2O exclusively have a significant late-barrier with a height around 20.5 kcal/mol. Considering the similarity of the MEPs of the three reactions, it is expected that the different reactivity of the H-abstraction and D-abstraction channels in the three reactions is possibly caused by the different mass combinations of the reactants. To verify the prediction, we perform quantum dynamics calculations on the HOOH PES by substituting the collider O with the atom H. Interestingly, the pseudo-reaction becomes to prefer the H-abstraction channel, like what has been found in the H + HOD reaction. Therefore, the different reactivity of the two channels in different reactions can be attributed, at least partly, to the different mass combinations.

For the abstraction reaction F + HOD, it favors the H-abstraction channel although the atom F is even heavier than the atom O. It appears that the above explanation cannot be applied to the reaction. However, in sharp contrast to the reactions H/Cl/O(^{3}P) + H_2O, the abstraction reaction F + H_2O possesses a very low early-barrier of 1.6 kcal/mol.[36] Thus, the reaction is considered to be very sensitive to the barrier height compared with the other three reactions. The lower vibrationally adiabatic barrier height for the H-abstraction channel in F + HOD reaction makes the H-abstraction reaction easier to happen.

TABLE IV. Isotope branching ratios of O′D:O′H in the O′ + HOD reaction except from the state (001). The values from the state (001) are given by the ratio of O′H:O′D.

E_{trans} (eV)	(000)	(010)	(100)	(020)	(001)
0.6	...	...	13.81	1.98	179.65
0.8	...	0.40	19.20	1.80	105.94
1.0	1.75	0.72	15.45	1.69	56.43
1.2	1.94	0.92	11.52	1.61	27.33
1.4	1.98	1.06	8.58	1.58	...
1.6	1.90	1.14	...	...	...

IV. CONCLUSIONS

The mode specificity, bond selectivity, and product branching ratio of the O′(^{3}P) + HOD abstraction reaction have been studied using a full-dimensional time-dependent quantum scattering method on the lowest triplet state PES of the HOOH system. It was found that on one hand vibrational excitation of three normal modes of the reactant HOD exclusively promotes the reaction. Both the H-abstraction channel and the D-abstraction channel prefer the vibrational energy to the translational energy except for vibrationally exciting the respective spectator bond. First overtone excitation of the bending mode of HOD presents a more notably promotional effect than what is expected from the fundamental excitation in the D-abstraction reaction. On the other hand, exciting the local stretching mode greatly increases the corresponding product yield, revealing a strong bond selectivity of the reaction. Furthermore, the bias to the D-abstraction products in the O′(^{3}P)/Cl + HOD reaction from the reactant ground state differs remarkably from what has been found in the H + HOD reaction, which is partially caused by the different mass combinations of the reactants. In sharp contrast, although the atom F is even heavier than the atom O, the H-abstraction

channel is favored in the F + HOD reaction due to a very low early-barrier.

ACKNOWLEDGMENTS

This work is supported by the National Natural Science Foundation of China (Grant Nos. 21603266 to H.S. and 11304095 to R.Z.).

[1]R. N. Zare, Science **279**, 1875 (1998).
[2]F. F. Crim, Proc. Natl. Acad. Sci. U. S. A. **105**, 12654 (2008).
[3]H. Guo and K. Liu, Chem. Sci. **7**, 3992 (2016).
[4]D. H. Zhang and H. Guo, Annu. Rev. Phys. Chem. **67**, 135 (2016).
[5]F. F. Crim, Acc. Chem. Res. **32**, 877 (1999).
[6]K. Liu, Annu. Rev. Phys. Chem. **67**, 91 (2016).
[7]J. C. Polanyi, Acc. Chem. Res. **5**, 161 (1972).
[8]J. C. Polanyi, Science **236**, 680 (1987).
[9]B. Jiang and H. Guo, J. Chem. Phys. **138**, 234104 (2013).
[10]H. Guo and B. Jiang, Acc. Chem. Res. **47**, 3679 (2014).
[11]M. J. Bronikowski, W. R. Simpson, B. Girard, and R. N. Zare, J. Chem. Phys. **95**, 8647 (1991).
[12]M. C. Hsiao, A. Sinha, and F. F. Crim, J. Phys. Chem. **95**, 8263 (1991).
[13]A. Sinha, M. C. Hsiao, and F. F. Crim, J. Chem. Phys. **94**, 4928 (1991).
[14]A. Sinha, J. D. Thoemke, and F. F. Crim, J. Chem. Phys. **96**, 372 (1992).
[15]R. B. Metz, J. D. Thoemke, J. M. Pfeiffer, and F. F. Crim, J. Chem. Phys. **99**, 1744 (1993).
[16]J. D. Thoemke, J. M. Pfeiffer, R. B. Metz, and F. F. Crim, J. Phys. Chem. **99**, 13748 (1995).
[17]M. J. Bronikowski, W. R. Simpson, and R. N. Zare, J. Phys. Chem. **97**, 2194 (1993).
[18]F. F. Crim, J. Phys. Chem. **100**, 12725 (1996).
[19]J. M. Pfeiffer, E. Woods, R. B. Metz, and F. F. Crim, J. Chem. Phys. **113**, 7982 (2000).
[20]K. Kudla and G. C. Schatz, Chem. Phys. Lett. **193**, 507 (1992).
[21]K. Kudla and G. C. Schatz, Chem. Phys. **175**, 71 (1993).
[22]D. Troya, M. González, and G. C. Schatz, J. Chem. Phys. **114**, 8397 (2001).
[23]D. C. Clary, Chem. Phys. Lett. **192**, 34 (1992).
[24]G. Nyman and D. C. Clary, J. Chem. Phys. **100**, 3556 (1994).
[25]J. R. Fair, D. Schaefer, R. Kosloff, and D. J. Nesbitt, J. Chem. Phys. **116**, 1406 (2002).
[26]X. Zhang, K. Han, and J. Z. H. Zhang, J. Chem. Phys. **116**, 10197 (2002).
[27]D. H. Zhang and J. C. Light, J. Chem. Soc. Faraday Trans. **93**, 691 (1997).
[28]B. Fu and D. H. Zhang, J. Phys. Chem. A **116**, 820 (2011).
[29]B. Fu and D. H. Zhang, J. Chem. Phys. **136**, 194301 (2012).
[30]B. Jiang and H. Guo, J. Am. Chem. Soc. **135**, 15251 (2013).
[31]B. Fu and D. H. Zhang, J. Chem. Phys. **138**, 184308 (2013).
[32]H. Song and H. Guo, J. Chem. Phys. **142**, 174309 (2015).
[33]J. Li, H. Song, and H. Guo, Phys. Chem. Chem. Phys. **17**, 4259 (2015).
[34]H. Song, S.-Y. Lee, Y. Lu, and H. Guo, J. Phys. Chem. A **119**, 12224 (2015).
[35]B. Fu and D. H. Zhang, J. Chem. Phys. **142**, 064314 (2015).
[36]J. Li, B. Jiang, H. Song, J. Ma, B. Zhao, R. Dawes, and H. Guo, J. Phys. Chem. A **119**, 4667 (2015).
[37]M. J. Redmon, G. C. Schatz, and B. C. Garrett, J. Chem. Phys. **84**, 764 (1986).
[38]M. Braunstein, R. Panfili, R. Shroll, and L. Bernstein, J. Chem. Phys. **122**, 184307 (2005).
[39]P. F. Conforti, M. Braunstein, B. J. Braams, and J. M. Bowman, J. Chem. Phys. **133**, 164312 (2010).
[40]B. J. Braams and J. M. Bowman, Int. Rev. Phys. Chem. **28**, 577 (2009).
[41]Z. Xie and J. M. Bowman, J. Chem. Theory Comput. **6**, 26 (2009).
[42]J. Li and H. Guo, J. Chem. Phys. **138**, 194304 (2013).
[43]J. Li, B. Jiang, and H. Guo, J. Chem. Phys. **139**, 204103 (2013).
[44]J. Li, R. Dawes, and H. Guo, Phys. Chem. Chem. Phys. **18**, 29825 (2016).
[45]B. Jiang and H. Guo, J. Chem. Phys. **139**, 054112 (2013).
[46]M. Braunstein and P. F. Conforti, Chem. Phys. Lett. **523**, 34 (2012).
[47]M. Braunstein and P. F. Conforti, J. Chem. Phys. **138**, 074303 (2013).
[48]D. H. Zhang and J. C. Light, J. Chem. Phys. **104**, 4544 (1996).
[49]J. Qi, D. Lu, H. Song, J. Li, and M. Yang, J. Chem. Phys. **146**, 124303 (2017).
[50]R. T Pack, J. Chem. Phys. **60**, 633 (1974).
[51]P. McGuire and D. J. Kouri, J. Chem. Phys. **60**, 2488 (1974).
[52]D. H. Zhang and S. Y. Lee, J. Chem. Phys. **110**, 4435 (1999).
[53]U. Manthe and F. Matzkies, J. Chem. Phys. **113**, 5725 (2000).
[54]D. H. Zhang, M. Yang, and S.-Y. Lee, J. Chem. Phys. **117**, 10067 (2002).
[55]F. Huarte-Larrañaga and U. Manthe, J. Chem. Phys. **118**, 8261 (2003).
[56]H. Song, Y. Lu, and S.-Y. Lee, J. Chem. Phys. **136**, 114307 (2012).
[57]H. Song, S.-Y. Lee, M. Yang, and Y. Lu, J. Chem. Phys. **139**, 154310 (2013).
[58]J. A. Fleck, Jr., J. R. Morris, and M. D. Feit, Appl. Phys. **10**, 129 (1976).
[59]D. Neuhasuer and M. Baer, J. Chem. Phys. **90**, 4351 (1989).
[60]W. H. Miller, S. D. Schwartz, and J. W. Tromp, J. Chem. Phys. **79**, 4889 (1983).
[61]D. H. Zhang and J. Z. H. Zhang, J. Chem. Phys. **99**, 5615 (1993).
[62]J. V. Lill, G. A. Parker, and J. C. Light, Chem. Phys. Lett. **89**, 483 (1982).
[63]J. Echave and D. C. Clary, Chem. Phys. Lett. **190**, 225 (1992).
[64]T. Shimanouchi, *Tables of Molecular Vibrational Frequencies Consolidated, Volume I* (National Bureau of Standards, Gaithersburg, MD, 1972).
[65]B. Zhao, U. Manthe, and H. Guo, Phys. Chem. Chem. Phys. **20**, 17029 (2018).